Inorg. Chem. **2004**, *43*, 3057–3066

Dyads Containing Iridium(III) Bis-terpyridine as Photoactive Center: Synthesis and Electron Transfer Study

Etienne Baranoff,[†] Isabelle M. Dixon,[†,§] Jean-Paul Collin,*[,†] Jean-Pierre Sauvage,*[,†] Barbara Ventura,[‡] and Lucia Flamigni*[,‡]

Laboratoire de Chimie Organo-Minérale, UMR 7513 CNRS, Université Louis Pasteur, Institut Le Bel, 4, rue Blaise Pascal, 67070 Strasbourg, France, and Istituto ISOF-CNR, Via P. Gobetti 101, 40129 Bologna, Italy

Received September 18, 2003

A series of Ir(III)–D dyads based on an iridium(III) bis-terpyridine complex as a photoactive center and tertiary amines as donor groups, as well as their individual components, have been designed to generate photoinduced charge separation. Depending on the donor group, a modular approach or a "chemistry-on-the-complex" approach has been used to prepare three different Ir(III)–D dyads. A detailed photophysical study has been performed on one Ir(III)–D dyad in which a triarylamine is linked to the iridium bis-terpyridine complex with an amido-phenyl group used as a spacer. In acetonitrile at room temperature, steady-state and time-resolved methods gave evidence of a photoinduced charge-separated state Ir^{-}–D^{+} with a lifetime of 70 ps. This relatively short lifetime could be due to the close proximity between the negative charge, likely localized in the bridging terpyridine, and the oxidized donor group.

Introduction

Photoinduced charge separation in multicomponent molecular systems is an important process modeling natural photosynthesis, in particular, the function of green plant or bacterial reaction centers. It is also promising in the field of the so-called artificial photosynthesis as a means to convert light energy into chemical energy.[1] Most of the systems are based on porphyrins as photoactive species, associated with electron donor and acceptor groups.[2−7] Besides this wide family of compounds, transition metal complexes have also been utilized as photoactive species in multicomponent compounds aimed at undergoing photoinduced charge separation.[8−10] Most of the transition metal centers leading to interesting photoactivity (electron transfer in the excited state versus chemical transformation) are d^6 metals,[11−13] although a few d^{10} systems (copper(I)) have recently been reported.[14−17] Ru(II)-containing complexes form the most

* To whom correspondence should be addressed. E-mail: sauvage@chimie.u-strasbg.fr (J.-P.S.); jpcollin@chimie.u-strasbg.fr (J.-P.C.); flamigni@isof.cnr.it (L.F.).

[†] Université Louis Pasteur.

[‡] Istituto ISOF-CNR.

[§] Present address: Laboratoire de Chimie de Coordination, UPR 8241 CNRS, Toulouse, France.

(1) Balzani, V.; Scandola, F. *Supramolecular Photochemistry*; Ellis Horwood: Chichester, U.K., 1991.
(2) Gust, D.; Moore, T. A.; Moore, A. L.; Lee, S. J.; Bittersmann, E.; Luttrull, D. K.; Rehms, A. A.; De Grazio, J. M.; Ma, X. C.; Gao, F.; Belford, R. E.; Trier, T. T. *Science* **1990**, *248*, 199.
(3) Imahori, H.; Guldi, D. M.; Tamaki, K.; Yoshida, Y.; Luo, C.; Sakata, Y.; Fukuzumi, S. *J. Am. Chem. Soc.* **2001**, *123*, 6617.
(4) Moore, T. A.; Gust, D.; Mathis, P.; Mialocq, J.-C.; Chachaty, C.; Bensasson, R. V.; Land, E. J.; Doizi, D.; Liddell, P.; Lehman, W. R.; Nemeth, G. A.; Moore, A. L. *Nature* **1984**, *307*, 630.
(5) Nishitani, S.; Kurata, N.; Sakata, Y.; Misumi, S.; Karen, A.; Okada, T.; Mataga, N. *J. Am. Chem. Soc.* **1983**, *105*, 7771.
(6) Osuka, A.; Zhang, R. P.; Maruyama, K.; Ohno, T.; Nozaki, K. *Chem. Lett.* **1993**, 1727.
(7) Wasielewski, M. R.; Niemczyk, M. P.; Svec, W. A.; Bradley-Pewitt, E. *J. Am. Chem. Soc.* **1985**, *107*, 5562.
(8) Balzani, V.; Juris, A.; Venturi, M.; Campagna, S.; Serroni, S. *Chem. Rev.* **1996**, *96*, 759.
(9) Meyer, T. J. *Acc. Chem. Res.* **1989**, *22*, 163.
(10) Sauvage, J.-P.; Collin, J.-P.; Chambron, J.-C.; Guillerez, S.; Coudret, C.; Balzani, V.; Barigelletti, F.; De Cola, L.; Flamigni, L. *Chem. Rev.* **1994**, *94*, 993.
(11) DeCola, L.; Belser, P. *Coord. Chem. Rev.* **1998**, *177*, 301.
(12) Scandola, F.; Indelli, M. T.; Chiorboli, C.; Bignozzi, C. A. *Top. Curr. Chem.* **1990**, *158*, 63.
(13) Sun, L.; Hammarström, L.; Åkermark, B.; Styring, S. *Chem. Soc. Rev.* **2001**, *30*, 36.
(14) Ichinaga, A. K.; Kirchhoff, J. R.; MacMillin, D. R.; Dietrich-Buchecker, C. O.; Marnot, P. A.; Sauvage, J.-P. *Inorg. Chem.* **1987**, *26*, 4290.
(15) Linke, M.; Chambron, J.-C.; Heitz, V.; Sauvage, J.-P.; Encinas, S.; Barigelletti, F.; Flamigni, L. *J. Am. Chem. Soc.* **2000**, *122*, 11834.
(16) Miller, M. T.; Karpishin, T. B. *Inorg. Chem.* **1999**, *38*, 5246.
(17) Scaltrito, D. V.; Thompson, D. W.; O'Callaghan, J. A.; Meyer, G. J. *Coord. Chem. Rev.* **2000**, *208*, 243.

10.1021/ic0351038 CCC: $27.50
Published on Web 04/20/2004

important class of such compounds,[18,19] Os(II)[20] and Re(I)[21,22] being also promising metal centers.

Another candidate with a d^6 electronic configuration is Ir(III). To the best of our knowledge, this metal center has almost never been incorporated as a photoactive species in multicomponent systems including other electroactive species.[23,24] Recently, $Ir(terpy)_2^{3+}$ (terpy = 2,2′;6′,2″-terpyridine) has been used as a gathering structural element and as an electron transfer relay in conjunction with a free base (PH_2) or a zinc porphyrin (PZn) electron donors in their singlet excited state, and a gold(III) porphyrin (PAu^+) as electron acceptor.[25−27] Upon selective excitation of the porphyrin donor in the visible wavelength, the following sequence of steps could be detected by time resolved spectroscopic determinations on the triad containing PZn, $Ir(terpy)_2^{3+}$, and PAu^+:

$$PZn-Ir(terpy)_2^{3+}-PAu^+ \xrightarrow{h\nu} {}^1PZn-Ir(terpy)_2^{3+}-PAu^+ \quad (1)$$

$${}^1PZn-Ir(terpy)_2^{3+}-PAu^+ \rightarrow PZn^+-Ir(terpy)_2^{2+}-PAu^+ \quad (2)$$

$$PZn^+-Ir(terpy)_2^{2+}-PAu^+ \rightarrow PZn^+-Ir(terpy)_2^{3+}-PAu^\bullet \quad (3)$$

The two electron-transfer steps (eqs 2 and 3) are followed by the charge recombination reaction, which leads back to the starting form of the triad $PZn-Ir(terpy)_2^{3+}-PAu^+$ in ~450 ns in toluene at room temperature.[26] Quite remarkably, upon selective excitation of the $Ir(terpy)_2^{3+}$ unit in the UV region of the spectrum, a switching of the photoinduced process to an energy transfer was seen in $PH_2-Ir(terpy)_2^{3+}-PAu^+$.[28]

Due to the particular electronic properties of $Ir(terpy)_2^{3+}$,[29−32] $Ir(diimine)_3^{3+}$, or their cyclometalated derivatives,[33−35] both in their ground state and in their LC or MLCT excited state, the use of such complexes as *photocenters* in D−Ir or D−Ir−A assemblies (D, electron donor; A, electron acceptor) is very attractive in view of generating charge separated states after direct excitation of the iridium(III) complex unit. It is worth noting that $Ir(terpy)_2^{3+}$ and its derivatives are powerful oxidants in their excited state and relatively good electron acceptors in their ground state.[29,30] In addition, the LC excited states are remarkably long-lived, especially for the complexes of terpy ligands substituted at the central 4′-position (up to 10 μs in CH_3CN, at room temperature). Combined with their chemical robustness, these electronic properties make $Ir(terpy)_2^{3+}$ derivatives promising complexes for photoinduced electron transfer in the presence of an electron donor. Moreover, it should be noted that the arrangement of bis-terpy complexes, with a well-defined axis running through the two central nitrogen atoms of the ligands and the metal center, allows precise control of the geometry of multicomponents systems such as dyads and triads.[10,36]

Results and Discussion

Design and Synthetic Strategy. The terpyridines **2** and **3** and the other appropriate derivatives **4**, **5**, **6**, and **7** are synthesized according to the equations shown in Scheme 1.

The already known 4′-aminophenyl-terpyridine **2** was obtained in good yield by reduction of the corresponding 4′-nitrophenyl-terpyridine **1**[37] with hydrazine and Pd on charcoal as a catalyst.[38] The terpyridine **3** was prepared by condensation of **2** with 4-dimethylaminobenzoic acid in the presence of DMAP and EDC (peptidic coupling, DMAP is dimethylamino-pyridine and EDC is *N*-(3-dimethylamino-propyl)-*N*′-ethylcarbodiimide hydrochloride).[39] An Ullman coupling of dianisylamine with the *p*-iodo-methylbenzoate afforded the dianisyl-methyl ester-phenylamine **4**, which was converted first to its acid derivative **5** and then to its acid chloride derivative **6**. This useful derivative was used to prepare the reference compound **7** and the iridium dyad $\mathbf{13}^{3+}$ (**Ir−D**) of Scheme 2.

For the synthesis of the iridium dyads, a modular approach (method A) was first investigated (Scheme 2), as previously reported for another family of iridium(III) complexes.[30]

The reaction of the precursor Ir(Ar-tpy)Cl_3 **8** (Ar = 3,5-di-*tert*-butylphenyl) with a terpyridine bearing a donor group (**3** or **9**[40]), in ethylene glycol at reflux, led to the dyads $\mathbf{10}^{3+}$ and $\mathbf{11}^{3+}$. However, in the harsh conditions used, the ligand **3** and the complex $\mathbf{11}^{3+}$ were subjected to a mono-demethylation of the amino unit. Because of the difficulty encountered in separating these side products, a "chemistry-on-the-complex" approach[41−43] was undertaken (method B). The key precursor $\mathbf{12}^{3+}$ obtained in good yield following the modular strategy allows the attachment of any chemical

(18) Johansson, O.; Borgström, M.; Lomoth, R.; Palmblad, M.; Bergquist, J.; Hammarström, L.; Sun, L.; Åkermark, B. *Inorg. Chem.* **2003**, *42*, 2908.
(19) Roundhill, D. M. *Photochemistry & Photophysics of Metal Complexes*; Plenum Press: New York, 1994.
(20) Collin, J.-P.; Guillerez, S.; Sauvage, J.-P.; Barigelletti, F.; DeCola, L.; Flamigni, L.; Balzani, V. *Inorg. Chem.* **1992**, *31*, 4112.
(21) Chen, P.; Westmoreland, T. D.; Danielson, E.; Schanze, K. S.; Anthon, D.; Neveux, P. E.; Meyer, T. J. *Inorg. Chem.* **1987**, *26*, 1116.
(22) Perkins, T. A.; Hauser, B. T.; Eyler, J. R.; Schanze, K. S. *J. Phys. Chem.* **1990**, *94*, 8745.
(23) Vogler, L. M.; Scott, B.; Brewer, K. J. *Inorg. Chem.* **1993**, *32*, 898.
(24) Fox, L. S.; Kozik, M.; Winkler, J. R.; Gray, H. B. *Science* **1990**, *247*, 1069.
(25) Dixon, I. M.; Collin, J.-P.; Sauvage, J.-P.; Barigelletti, F.; Flamigni, L. *Angew. Chem., Int. Ed.* **2000**, *39*, 1292.
(26) Dixon, I. M.; Collin, J.-P.; Sauvage, J.-P.; Flamigni, L. *Inorg. Chem.* **2001**, *40*, 5507.
(27) Flamigni, L.; Dixon, I. M.; Collin, J.-P.; Sauvage, J.-P. *Chem. Commun.* **2000**, 2479.
(28) Flamigni, L.; Marconi, G.; Dixon, I. M.; Collin, J.-P.; Sauvage, J.-P. *J. Phys. Chem. B* **2002**, *106*, 6663.
(29) Ayala, N. P.; Flynn, C. M.; Sacksteder, L.; Demas, J. N.; DeGraff, B. A. *J. Am. Chem. Soc.* **1990**, *112*, 3837.
(30) Collin, J.-P.; Dixon, I. M.; Sauvage, J.-P.; Williams, J. A. G.; Barigelletti, F.; Flamigni, L. *J. Am. Chem. Soc.* **1999**, *121*, 5009.
(31) Licini, M.; Williams, J. A. G. *Chem. Commun.* **1999**, 1943.
(32) Lo, K. K.-W.; Chung, C.-K.; Ng, D. C.-M.; Zhu, N. *New. J. Chem.* **2002**, *26*, 81.
(33) Dixon, I. M.; Collin, J.-P.; Sauvage, J.-P.; Flamigni, L.; Encinas, S.; Barigelletti, F. *Chem. Soc. Rev.* **2000**, *29*, 385.
(34) Lo, K. K.-W.; Chung, C.-K.; Zhu, N. *Chem. Eur. J.* **2003**, *9*, 475.
(35) Watts, R. J. *Comments Inorg. Chem.* **1991**, *11*, 303.
(36) Collin, J.-P.; Guillerez, S.; Sauvage, J.-P. *Chem. Commun.* **1989**, 776.
(37) Mukkala, V.-M.; Helenius, M.; Hemmilä, I.; Kankare, J.; Takalo, H. *Helv. Chim. Acta* **1993**, *76*, 1361.
(38) Ishow, E.; Gourdon, A.; Launay, J.-P.; Chiorboli, C.; Scandola, F. *Inorg. Chem.* **1999**, *38*, 1504.
(39) Sheehan, J. C.; Cruickshank, P. A.; Boshart, G. L. *J. Org. Chem.* **1961**, *26*, 2525.
(40) Collin, J.-P.; Guillerez, S.; Sauvage, J.-P.; Barigelletti, F.; DeCola, L.; Flamigni, L.; Balzani, V. *Inorg. Chem.* **1991**, *30*, 4230.

Scheme 1. Synthesis of the Organic Molecules

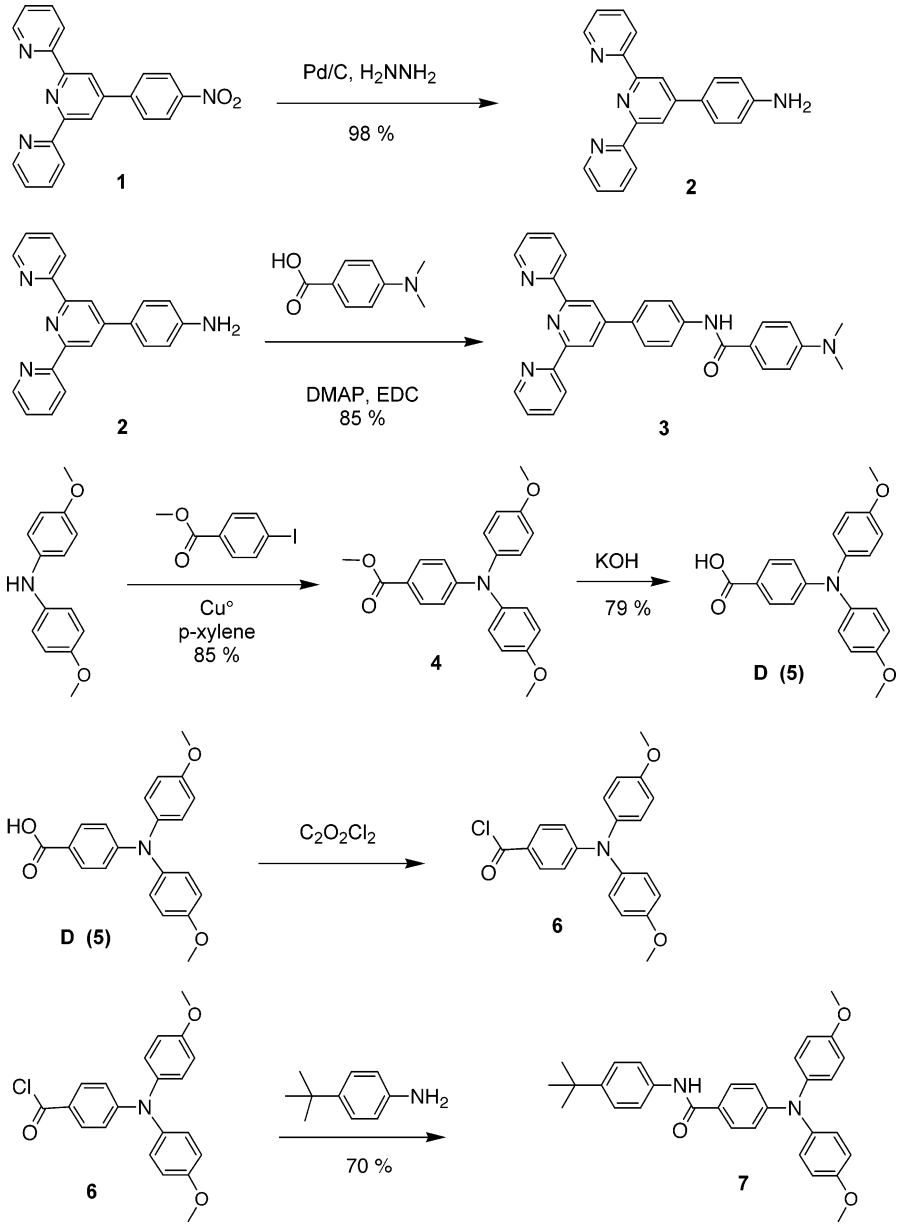

group bearing an acid chloride function. The diad $\mathbf{13}^{3+}$ and the reference compound $\mathbf{14}^{3+}$ were synthesized in a straightforward manner by reaction of $\mathbf{12}^{3+}$ with **6** or benzoyl chloride, which resulted in 60% and 64% yield, respectively.

Electrochemistry. The redox characteristics of the dyads $\mathbf{10}^{3+}$, $\mathbf{11}^{3+}$, **Ir**−**D** ($\mathbf{13}^{3+}$), and the reference compounds **D**, **7**, and **Ir**−**1** (see Scheme 3) examined by cyclic voltammetry in CH_3CN are reported in Table 1.

Reversible monoelectronic waves were observed for all redox processes and assigned by comparison with the values of the redox potentials of the reference compounds. The oxidation of the tertiary amine unit in $\mathbf{11}^{3+}$ is more difficult (by 300 mV) than in the other dyads reflecting the electronic effect of the two methyl groups. In dyad $\mathbf{10}^{3+}$, the redox potential of the arylamine unit is also shifted to the positive range (60 mV) due to the close proximity of the two electroactive groups. Concerning the first and second reduction of the terpyridine ligand in these complexes, only minor potential shifts are observed. Except for dyad $\mathbf{10}^{3+}$, weak donor−acceptor interactions are indicated by the values of the different redox couples. Therefore, the usual approach based on a localized description of the individual components seems reasonable.

Ground-State Absorption Spectra. Absorption spectra of multicomponent structures are diagnostics of electronic coupling occurring between components. The absorption spectra of the dyads $\mathbf{10}^{3+}$, $\mathbf{11}^{3+}$ and of the model compound **Ir**−**1** in acetonitrile are shown in Figure 1. As compared to the model **Ir**−**1**, the position of the low energy transition of dyad $\mathbf{11}^{3+}$ is red-shifted by about 60 nm indicating a

(41) Chodorowski-Kimmes, S.; Beley, M.; Collin, J.-P.; Sauvage, J.-P. *Tetrahedron Lett.* **1996**, *37*, 2963.
(42) Storrier, G. D.; Colbran, S. B.; Craig, D. C. *J. Chem. Soc., Dalton Trans.* **1997**, 3011.
(43) Tzalis, D.; Tor, Y. *J. Am. Chem. Soc.* **1997**, *119*, 852.

Scheme 2. Synthesis of the Complexes

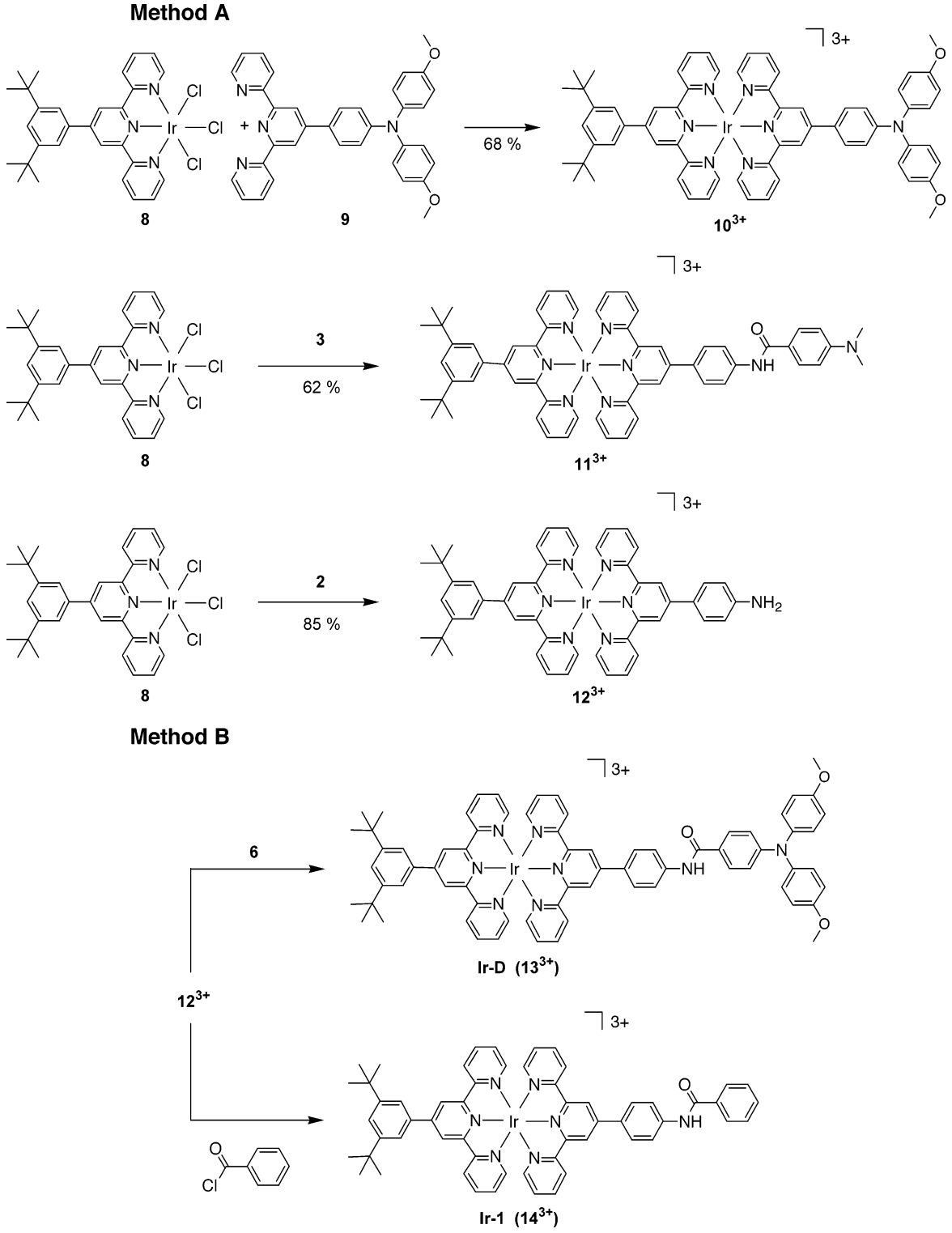

noticeable interaction between the two components. This effect is drastically enhanced for dyad $\mathbf{10}^{3+}$ in which a broad, stabilized intramolecular charge transfer band appears at 506 nm. Predictably,[41] compound $\mathbf{10}^{3+}$ is strongly solvatochromic: the absorption maximum undergoes a significant blue shift as the solvent polarity increases from CH_2Cl_2 (λ_{max} = 557 nm) to DMSO (λ_{max} = 499 nm). This negative solvatochromism can be explained by the smaller dipole moment in the excited charge transfer (CT) state than in the ground state. This phenomenon is well documented and has been observed in several cases.[44−46] As a consequence, the large electronic coupling in $\mathbf{10}^{3+}$ precludes the observation of any emission band in CH_3CN.[47]

(44) Curtis, J. C.; Sullivan, B. P.; Meyer, T. J. *Inorg. Chem.* **1983**, *22*, 224.
(45) Chen, C.-T.; Liao, S.-Y.; Lin, K.-J.; Chen, C.-H.; Lin, T.-Y. J. *Inorg. Chem.* **1999**, *38*, 2734.
(46) Knör, G.; Leirer, M.; Keyes, T. E.; Vos, J. G.; Vogler, A. *Eur. J. Inorg. Chem.* **2000**, 749.

Scheme 3. Components Which Have Been Photophysically Investigated

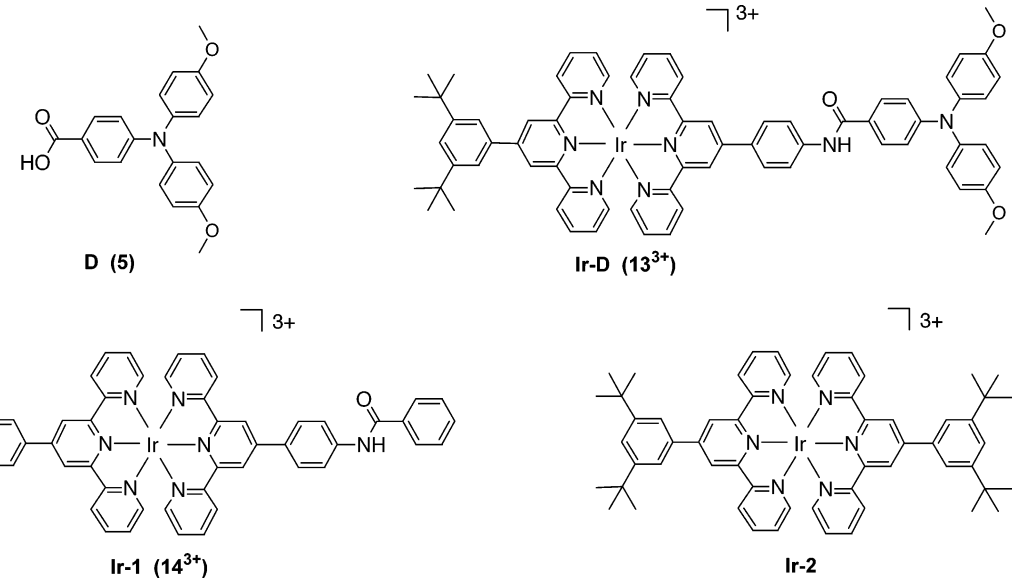

Table 1. Cyclic Voltammetry Data of the Dyads $\mathbf{10}^{3+}$, $\mathbf{11}^{3+}$, and **Ir**−**D** and the Reference Compounds **D**, **7**, **Ir**−**1**, and **Ir**−**2** in MeCN, 0.1 M nBu$_4$NPF$_6$, with SCE as Reference

	$E_{1/2}$ (V vs SCE)		
	NR_3^+/NR_3	terpy/terpy$^-$	terpy$^-$/terpy^{2-}
D	0.80		
7	0.73		
Ir-1		−0.76	−0.92
Ir-2		−0.74	−0.92
$\mathbf{10}^{3+}$	0.79	−0.76	−0.90
$\mathbf{11}^{3+}$	1.02	−0.75	−0.86
Ir-D	0.75	−0.76	−0.92

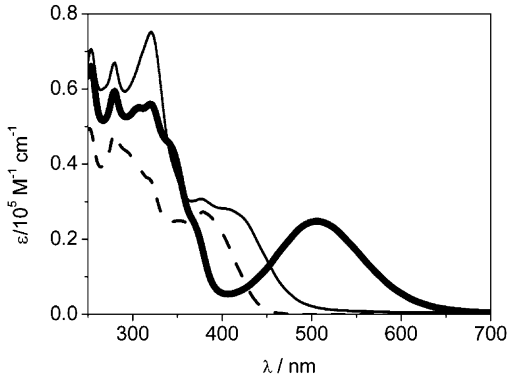

Figure 1. Molar absorption coefficients in acetonitrile solutions of the components **Ir**−**1** ($\mathbf{14}^{3+}$) (dashed line), $\mathbf{10}^{3+}$ (bold solid line), and $\mathbf{11}^{3+}$ (solid line).

Due to the noticeable interaction in conjunction with some photolability detected in dyad $\mathbf{11}^{3+}$, and to the remarkable charge transfer interaction detected in dyad $\mathbf{10}^{3+}$, the photophysical studies of these structures were not carried out. In such strongly coupled multicomponent systems, the processes are expected to be extremely fast.

The dyad **Ir**−**D** ($\mathbf{13}^{3+}$) was, however, found suitable for a detailed photophysical investigation with our experimental resolution (20−30 ps), and the results are illustrated in the following sections. Scheme 3 summarizes the dyad and the

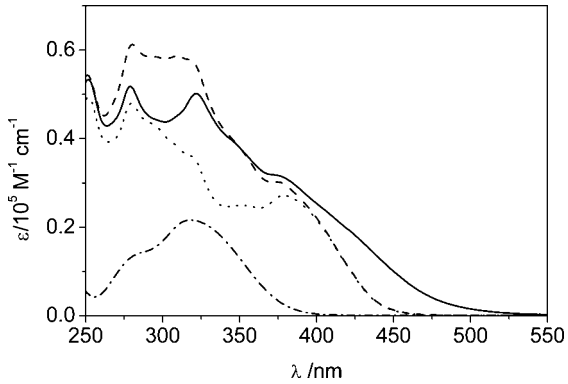

Figure 2. Molar absorption coefficients in acetonitrile solutions of the components **Ir**−**1** (···) and **D** (− · −) compared to the molar absorption coefficients of **Ir**−**D** (−) and to the sum of the components (- - -).

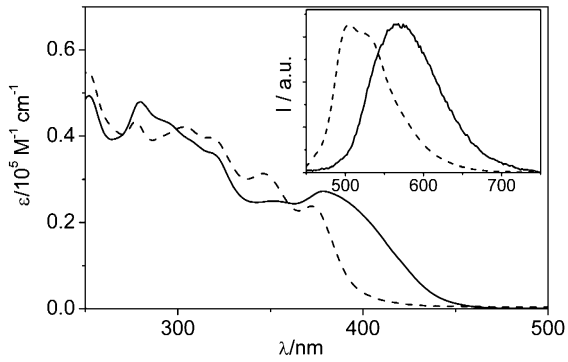

Figure 3. Comparison of molar absorption coefficients in acetonitrile solutions of the complexes **Ir**−**2** (- - -) and **Ir**−**1** (−). In the inset, the normalized emission at 298 K is reported.

model components that have been photophysically investigated. The absorption spectra in acetonitrile of the electron donor **D**, of **Ir**−**1**, and of **Ir**−**D** appear in Figure 2. With respect to the symmetrically substituted Ir(3,5-di-*tert*-butylphenyl)$_2$ complex (**Ir**−**2**, Scheme 3) previously reported,[30] the present **Ir**−**1** complex displays a red shifted absorption band (λ_{max} = 383 nm), as shown in Figure 3. The lower energy band in **Ir**−**1**, compared to **Ir**−**2**, has to be ascribed to the transition to a more stabilized state due to the presence

(47) Reichardt, C. *Chem. Soc. Rev.* **1992**, 147.

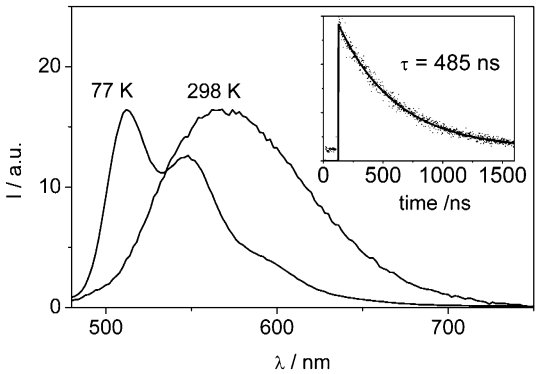

Figure 4. Luminescence properties at 77 K (butyronitrile) and 298 K (acetonitrile) of the complex **Ir−1**. In the inset, the luminescence data and exponential fitting measured upon excitation at 337 nm are reported.

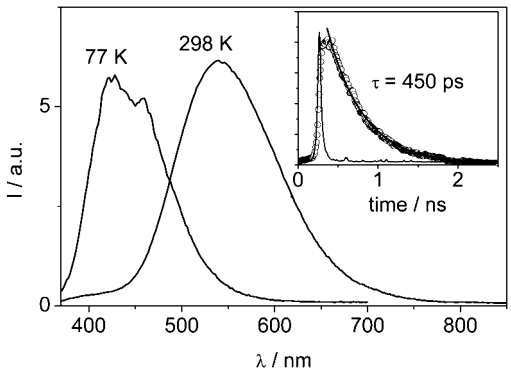

Figure 5. Luminescence properties at 77 K (butyronitrile) and 298 K (acetonitrile) of the donor **D**. In the inset, the luminescence data and exponential fitting upon excitation at 355 nm are reported with the excitation profile.

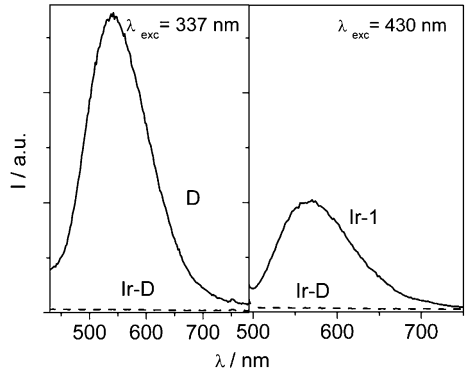

Figure 6. Luminescence intensity from optically matched acetonitrile solutions of (left panel) **D** and **Ir−D** and (right panel) of **Ir−1** and **Ir−D**.

of the phenyl-amide substitutent on the terpy ligand. The absorption spectrum of the array **Ir−D** agrees well with a simple superposition of the spectra of the single components, except for a slight broadening in the 450−500 nm region. The modest shift can be assigned to a further stabilization in energy of the band localized on the phenyl-amide substituted ligand of the iridium complex when the donor unit is covalently bonded. The spectra reported in Figure 2 allow one to establish the partition of photons absorbed by the different units of the dyad for the excitation wavelength. At a wavelength longer than 400 nm, a selective excitation of the iridium moiety is achieved in the dyad, whereas at 355 nm, a wavelength convenient for laser excitation, 70% of the photons are absorbed by the Ir unit and 30% by the D unit.

Luminescence. The luminescence spectrum of **Ir−1** in acetonitrile solution at 298 K displays a maximum at 570 nm, red shifted and less structured than the one corresponding to **Ir−2** (inset of Figure 3). At 77 K, the experiment performed in butyronitrile, to provide a high quality glass, displays an emission spectrum with some structure and a shift to higher energy (λ_{max} = 510 nm) (Figure 4). The emission quantum yield at 298 K (see Experimental Section for details) is 3.5×10^{-3}, much lower than that of **Ir−2** (ϕ_{em} = 0.022) and similar complexes previously studied.[30] In that case, the nature of the lowest emitting excited state for a series of Ir bis-terpyridine type complexes was assigned as a ligand centered triplet, ^{3}LC. The assignment was rather clear for the simplest Ir(2,2′;6′,6″-terpyridine)$_2$ complex, whereas in the substituted terpyridine complexes, as in bis-tolylterpyridine or bis-di-tertiobutylterpypiridine derivative, some mixing with metal to ligand excited triplet state, ^{3}MLCT, was not excluded. Stabilization of MLCT excited states by protonation in an Ir(III) bis-terpyridine complex incorporating a pendent pyridyl group confirmed that mixing of MLCT with LC states can lead to a red shift in absorption, a decrease in luminescence quantum yield, and a decrease in the lifetime of the excited state.[31] In agreement with this, the present case can be interpreted either as an emission from a ^{3}LC centered state strongly mixed with stabilized ^{3}MLCT excited states or as a ^{3}MLCT state.

The luminescence decay of **Ir−2** in air equilibrated acetonitrile solution was measured by a single photon time correlation apparatus and was fitted by a single exponential with a τ = 485 ns, shown as a continuous line in the inset of Figure 4. In air purged acetonitrile, the lifetime is 1.2 μs, yielding a rate of reaction of the excited state of the complex (^{3}Ir) with molecular oxygen of the order of 7×10^8 $M^{-1}\cdot s^{-1}$,[48] in agreement with the literature.[29,30]

The component **D** emits rather strongly at room temperature (ϕ_{em} = 0.012) with a maximum at 540 nm; in glassy butyronitrile at 77 K the emission maximum shifts to 422 nm (Figure 5). The large Stokes shift detected in the emission at room temperature of **D**, and the large temperature effect resulting in a destabilization in rigid media of the emitting state could be associated with a strongly distorted excited state with charge transfer character, as reported for several substituted amines.[49] The luminescence decay of **D** following excitation at 355 nm is measured by a streak camera and is fitted by a single exponential with a lifetime of 450 ps (inset of Figure 5).

In the dyad **Ir-D**, the luminescence of both components is totally quenched, as shown in Figure 6. In the left panel the luminescence from optically matched solutions of the **D** model and of **Ir−D** excited at 337 nm is reported, and in the right panel, the luminescence of **Ir−1** model is compared to that of **Ir−D** after selective excitation at 430 nm. Time-

(48) Murov, S. L.; Carmichael, I.; Hugh, G. L. *Handbook of Photochemistry*; Marcel Dekker Inc.: New York, 1993.
(49) Grabowski, Z. R.; Rotkiewicz, K.; Siemiarczuk, A.; Cowley, D. J.; Baumann, W. *Nouv. J. Chim.* **1979**, *3*, 443.

Table 2. Luminescence Properties and Energy Levels of the Excited States in Air Equilibrated Solutions of **Ir−D** and Models in Nitriles[a]

		298 K			77 K	
	state	λ_{max} (nm)	τ (ns)	Φ_{em}[b]	λ_{max} (nm)	E (eV)[c]
Ir−2[d]	^{3}Ir	506	1600	0.022	486	2.55
Ir−1[e]	^{3}Ir	570	485	3.5×10^{-3}	510	2.43
D[f]	^{1}D	540	0.450	0.012	422	2.93
Ir−D[g]	^{3}Ir−D		≤0.02	$\leq 6 \times 10^{-5}$	515[h]	2.45
	Ir−^{1}D			$\leq 6 \times 10^{-5}$		

[a] Acetonitrile at 298 K, butyronitrile at 77 K. [b] Emission quantum yields in air equilibrated acetonitrile; see Experimental Section for details. [c] Energy levels from the emission maxima at 77 K. [d] From ref 30. [e] Excitation of Ir unit at 378 nm for steady state; for time resolved experiments, excitation at 337 nm. [f] Excitation of D unit at 337 nm for steady state; for time resolved determinations, excitation at 355 nm. [g] Excitation of Ir unit at 430 nm and of D unit at 337 nm; time resolved excitation was either at 337 or 355 nm. [h] Weak signal.

resolved luminescence studies following excitation at 355 nm of the **Ir−D** dyad by an apparatus with 20 ps resolution do not indicate any residual detectable luminescence either for **D** or for **Ir−1** components. For the latter, the low radiative rate constant ($k_{rad} = \phi_{em}/\tau = 7.2 \times 10^3$ s^{-1}) could prevent detection by means of single pulse experiments as the present one, without implying a lifetime shorter than the 20 ps resolution. On the contrary, for the **D** component, characterized by a high radiative rate constant ($k_{rad} = 2.6 \times 10^7$ s^{-1}), the failure to detect any short-lived luminescence at 540 nm is a clear indication that the quenching occurs with a lifetime faster than the experimental resolution, i.e., with $k \geq 5 \times 10^{10}$ s^{-1}.

The results of luminescence determinations are summarized in Table 2.

Transient Absorbance. This technique, in addition to spectral and kinetic information on the excited states, allows us to derive information on any other intermediate. Since we are interested in the electron transfer occurring upon light irradiation, which is expected to yield the reduced form of the metal complex electron acceptor (Ir^-) and the oxidized radical of the donor **D** (D^+), valuable information can be gained. In order to help the characterization of the radicals produced by electron transfer, the oxidized form of **7**, which one can consider as a model of the oxidized form of **D**, i.e. D^+, was produced by chemical oxidation using Br_2 in acetonitrile (see Experimental Section for details). The resulting spectrum, with a peak at 760 nm and a minor band at 590 nm, is reported in Figure 7.

The excited state of **Ir−1** in air equilibrated acetonitrile displays a strong absorption spectrum with a broad maximum around 780 nm, as detected after excitation at 355 nm with a 35 ps laser pulse (Figure 8). During the time window of this experiment (3.3 ns), there is essentially no decay of the state, but its lifetime can be derived by performing a nanosecond laser flash-photolysis experiment (data not shown), where a lifetime of 440 ns is measured, in agreement with the luminescence lifetime of 485 ns (Table 3). The coincidence, within experimental errors, with the luminescence lifetime indicates that the absorbing excited state is also responsible for the emission. It should be mentioned

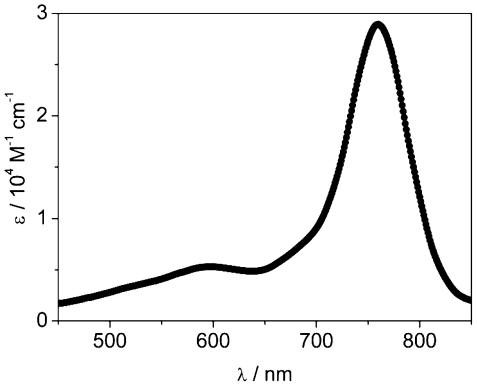

Figure 7. Spectrum of 7^+ chemically generated by addition of Br_2.

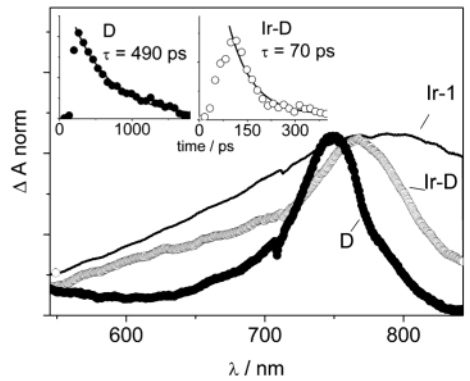

Figure 8. Normalized transient absorption spectra registered at the end of a 35 ps pulse (355 nm, 3 mJ/pulse) of acetonitrile solutions of **Ir−1**, **D**, and **Ir−D**. In the insets the absorbance decays corresponding to **D** and **Ir−D** are reported with the exponential fittings.

Table 3. Transient Absorbance in Air Equilibrated Acetonitrile Solutions at 298 K of Ir−D and Models Following Excitation at 355 nm

	298 K		
	state	λ_{max} (nm)	τ (ns)
Ir−2[a]	^{3}Ir	670	1650
Ir−1	^{3}Ir	780	440
D	^{1}D	750	0.490
Ir−D	^{3}Ir−D	780	≤0.02
	Ir^--D^+	765	0.070

[a] From reference.[30]

that the transient absorbance band of the symmetric reference compound **Ir−2** displayed a broad maximum at 670 nm.[30]

The transient absorbance spectrum detected at the end of a 355 nm, 35 ps laser pulse for **D** in acetonitrile is reported in Figure 8 and shows a sharp band with a maximum at 749 nm. The decay of this absorbance occurs with a lifetime of 490 ps, inset of Figure 8, in agreement with the luminescence decay and is, therefore, assigned to the singlet excited state of **D**, ^{1}D.

The end of the pulse spectra detected in an acetonitrile solution containing **Ir−D** is reported in Figure 8. There is no clear residual absorbance that can be ascribed to the Ir complex. Therefore, the quenching of this unit is believed to occur with a lifetime ≤20 ps, the instrumental resolution. The end of pulse spectrum in the dyad displays a band at 765 nm, with a broad shoulder between 570 and 700 nm. The spectrum, very similar to the one of the oxidized donor model **7** determined by an independent experiment (Figure

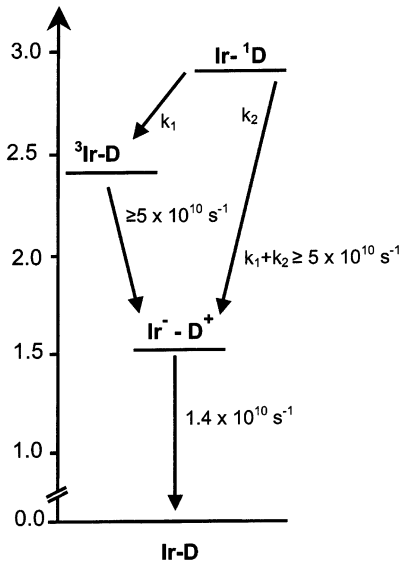

Figure 9. Schematic energy level diagram of photoinduced processes in **Ir**−**D**.

7), is assigned to the charge separated state Ir^--D^+. The decay of the charge separated state (CS) takes place with a lifetime of 70 ps, as shown in the inset of Figure 8.

The results of transient absorption experiments are summarized in Table 3.

Photoinduced Processes. From the reduction potential of the Ir complex unit in the dyad **Ir**−**D**, −0.75 V, and the oxidation potential of the donor in the same array, +0.76 V, it is possible to derive an approximate energy of 1.5 eV for the charge separated state Ir^--D^+, where an extra electron is localized on the metal complex, most probably on the bridging ligand, and a hole is on the donor. The luminescence experiments (Table 2) indicate that the energy levels of the excited states localized on the Ir complex and on the donor unit have an energy of ca. 2.4 and 2.9 eV, respectively. Therefore, an electron transfer process is thermodynamically possible upon excitation of either unit (Figure 9). To support this, a quenching of the luminescent states localized on either unit can be detected, as reported in Figure 6. Nonetheless, in the case where the higher energy donor unit is excited (2.9 eV), an energy transfer to the triplet metal complex component cannot be excluded (Figure 9). This could take place either via the singlet manifold excited state of the metal complex or directly to the triplet due to the spin−orbit perturbation induced by the heavy iridium metal ion.

Assuming that quenching of both excited states (^{3}Ir−D or Ir−^{1}D) is due to electron transfer, the mechanism can be described as follows. In the case where the Ir complex is excited, a reductive quenching of its excited state will occur; i.e., the electron will move from the HOMO localized on the donor to the HOMO localized on the Ir complex. Whereas in the case where the donor is excited, an electron will move from the LUMO localized on the donor to the LUMO on the Ir complex acceptor. The product will be in both cases the charge separated state $Ir^- -D^+$. The $\Delta G°$ of the reaction will be of the order of −0.9 eV when the initial state is ^{3}Ir−D or −1.4 eV when the initial state is Ir−^{1}D.

Time-resolved luminescence experiments indicate that, upon excitation at 355 nm, the lifetime of the excited donor which is easily observed in the model **D** with a lifetime of 450 ps is reduced to a value lower than the instrumental resolution of 20 ps. On the other hand, transient absorption spectroscopy indicates that at the end of the picosecond pulse the spectrum in the dyad **Ir**−**D** has no trace of the ^{3}Ir component, but it is identical to the D^+ species, indicating that the electron transfer has taken place within the experimental resolution of 20 ps. This allows us to place lower limits of 5×10^{10} s^{-1} for the charge separation step. The Ir^--D^+ charge separated species rapidly formed, characterized by a spectrum reminiscent of that of D^+, decays back to the ground state with a lifetime of 70 ps. After it decays, no residual absorbance is left which could be ascribed to other intermediates. The charge recombination step is characterized by a $\Delta G° = -1.5$ eV, strongly exoergonic. The high driving force could place the recombination reaction in the so-called "Marcus inverted region" characterized by a decrease in rate with increase in driving force.[50] Nonetheless, the charge recombination is still rather fast in the tens of picoseconds region. The close proximity of the extra electron, very likely residing in the bridging terpyridine ligand, to the positive charge could be the reason for the high recombination rate. Furthermore, the high inner reorganization energy value (λ_i)[50] associated with the present amine, which is expected to have a rather important change in geometry from the cationic to the neutral form, could contribute to increase the overall reorganization energy of the system with the consequence of shifting the inverted region to more negative $\Delta G°$.

This dyad could be regarded as a promising building block for the construction of more complex arrays including electron acceptors able to undergo multistep electron transfer, and we are presently working along that direction in order to increase the separation between the hole and the electron in the final charge separated state.

Experimental Section

Synthesis. General Procedures. The following chemicals were obtained commercially and used without further purification: KPF_6 (Avocado), *p*-iodo methylbenzoate (Avocado), oxalyl chloride (Accros), benzoyl chloride (Fluka), *p*-dimethylaminobenzoic acid (Acros), DMAP (Acros), EDC (Acros).

Equipment and Methods. ^{1}H NMR spectra were acquired either on a Bruker WP200 SY, a Bruker AC300, or a Bruker AM400 spectrometer, using the deuterated solvent as the lock and residual solvent as the internal reference. Mass spectra were obtained by using a VG ZAB-HF spectrometer (FAB), a Fisons VG Platform (ES), or a Fisons VG Trio 2000 (EI) spectrometer. Cyclic voltammetry experiments were performed using an EG&G 273A potentiostat, a Pt working electrode, a Pt counterelectrode, a saturated calomel electrode (SCE), 0.1 M nBu$_4$NPF$_6$ as supporting electrolyte, and MeCN as solvent.

Starting Compounds. 4′-*p*-Nitrophenyl-2,2′;6′,2″-terpyridine,[37] ^{t}ButpyIrCl$_3$,[30] 4,4′-dimethoxy-diphenylamine,[51] and bis(4-methox-

(50) Marcus, R. A.; Sutin, N. *Biochim. Biophys. Acta* **1985**, *811*, 265.
(51) Wolfe, J. P.; Tomori, H.; Sadighi, J. P.; Yin, J.; Buchwald, S. L. *J. Org. Chem.* **2000**, *65*, 1158.

yphenyl)(4-[2,2′;6′,2″]terpyridin-4′-ylphenyl)amine[40] were prepared according to the published procedures.

***p*-Anilino-2,2′;6′,2″-terpyridine (tpy-Ph-NH$_2$) (2).** tpy-Ph-NO$_2$ (3 g, 8.5 mmol) was dissolved in refluxing EtOH/THF (375 mL/375 mL). Pd/C (1.25 g) (10%) was added as a solid, and hydrazine monohydrate (10.2 mL) was added dropwise over a period of 15 min. After additional 15 min at reflux, the solution was filtered over Celite and evaporated to dryness. The solid was recristallized from EtOH. After filtration and drying under vacuum, **2** was obtained as a slightly yellow solid. Yield 87% (2.39 g). ^{1}H NMR (DMSO-d_6; 300 MHz): δ 8.76 (bd, 2H, H$_{66''}$, ^3J = 4.8 Hz); 8.65 (d, 2H, H$_{33''}$, ^3J = 7.6 Hz); 8.63 (s, 2H, H$_{3'5'}$); 8.02 (dt, 2H, H$_{44''}$, ^3J = 7.6 Hz, ^4J = 1.8 Hz); 7.68 (d, 2H, H$_{o1}$, ^3J = 8.6 Hz); 7.52 (ddd, 2H, H$_{55''}$, ^3J = 7.5 Hz, ^3J = 4.9 Hz, ^4J = 1.1 Hz); 6,75 (d, 2H, H$_{m1}$, ^3J = 8.6 Hz); 5.60 (bs, 2H, NH$_2$). ^{13}C NMR (DMSO-d_6, 75 MHz): δ 155.4, 155.3, 150.5, 149.5, 149.2, 137.3, 127.6, 124.3, 123.8, 120.8, 116.2, 114.3.

Terpy-Ph-NHCO-Ph-NMe$_2$ (3). 4-(Dimethylamino)benzoic acid (153 mg, 0.926 mmol, 1.5 equiv) was placed in a 25-mL two-necked flask. Distilled CH_2Cl_2 (2 mL) was added via cannula. DMAP (226 mg, 1.852 mmol, 3 equiv) and EDC (207 mg, 1.08 mmol, 1.75 equiv) were added. Separately, in a second 25-mL two-necked flask was placed **2** (200 mg, 0.617 mmol). Distilled CH_2Cl_2 (8 mL) was added through cannula. This suspension was transferred into the first (reaction) flask, and the second flask was washed 4 times with 3 mL of solvent. The reaction took place in 22 mL of solvent total. This mixture was stirred at room temperature, under argon, and in the dark for 24 h, after which it was washed with 5% $NaHCO_3$ (2 $\times$ 50 mL) and H_2O (100 mL). The crude mixture was evaporated and dissolved in CH_2Cl_2. The insoluble portion was filtered off and recrystallized in hot $CHCl_3$. NMR permitted identification of the crystals as pure **3** (183 mg, 63%). ^{1}H NMR ($CDCl_3$ + CD_3OD, 200 MHz): δ 8.55−8.30 (m, 6H, H$_{3'5'}$H$_{66''}$H$_{33''}$); 7.75−7.57 (m, 8H, H$_{o1}$H$_{m1}$H$_{o2}$H$_{44''}$); 7.21−7.13 (m, 2H, H$_{55''}$); 6.48 (d, 2H, H$_{m2}$, ^3J = 9.1 Hz); 4.97 (s, 1H, NH); 2.79 (s, 6H, CH_3). MS (FAB$^+$), *m*/*z*: 472.3 [M + H]$^+$. UV−vis (CH_3CN), λ_{max}/nm (ϵ/M^{-1} cm^{-1}): 203 (19500), 227 (10100), 252 (7000), 286sh (11500), 331 (15900).

4-(*N*,*N*-Bis(4-methoxy-phenyl)amino)methylbenzoate (4). The method used is similar to those described previously for analogous compounds.[52] 4,4′-Dimethoxydiphenyl-amine (5.23 g, 22.8 mmol), *p*-iodo methylbenzoate (6.01 g, 22.9 mmol), dry K_2CO_3 (3.71 g), copper bronze (1.16 g), 1.5 mL of *p*-xylene, and a small iodine crystal were heated at 200 °C under argon and protected from light for 24 h. When the solution was at room temperature, ether was added. The precipitate was filtered through a Büchner funnel and washed with ether. The filtrate was evaporated, and the oil obtained was chromatographed on silica with CH_2Cl_2. Compound **4** was obtained as a very viscous yellow oil. Yield 85% (7.1 g). ^{1}H NMR ($CDCl_3$, 300 MHz): δ 7.77 (d, 2H, H$_{o1}$, ^3J = 9 Hz); 7.03 (d, 4H, H$_a$, ^3J = 9 Hz); 6.79 (d, 6H, H$_b$+ H$_{m1}$, ^3J = 9 Hz); 3.75 (s, 3H, CH$_{3met}$); 3.67 (s, 6H, CH_3). ^{13}C NMR ($CDCl_3$, 75 MHz): δ 166.3, 156.5, 152.2, 138.9, 130.4, 127.3, 119.8, 116.9, 114.5, 54.8, 51.0.

4-(*N*,*N*-Bis(4-methoxy-phenyl)amino)methylbenzoic Acid (5). Compound **4** (7.1 g, 19.5 mmol) was heated at 130 °C for 2 h in 90 mL of 10% KOH solution. The solution was then acidified until the pH reached 5, and the precipitate was filtered. The precipitate was chromatographed on thick silica with CH_2Cl_2 followed by ether. The acid was obtained as a yellow solid. Yield: 79% (5.42 g). ^{1}H NMR ($CDCl_3$, 300 MHz): δ 7.77 (d, 2H, H$_{o2}$, ^3J = 9 Hz); 7.03 (d, 4H, H$_a$, ^3J = 9 Hz); 6.79 (d, 6H, H$_b$H$_{m2}$, ^3J = 9 Hz); 3.75 (s, 3H, CH$_{3met}$); 3.67 (s, 6H, CH_3). ^{13}C NMR ($CDCl_3$, 75 MHz): δ 166.3, 156.5, 152.2, 138.9, 130.4, 127.3, 119.8, 116.9, 114.5, 54.8, 51.0.

4-(*N*,*N*-Bis(4-methoxy-phenyl)amino)methylbenzoyl Chloride (6). Compound **5** (210 mg, 0.6 mmol) was dissolved in 10 mL of freshly distilled CH_2Cl_2. A few drops of pyridine were added, and the yellow solution was heated until reflux. Then, oxalyl chloride (0.25 mL) was added, and the solution was allowed to reflux for 2 h under argon. Another 0.25 mL of oxalyl chloride was added, and the mixture was refluxed for another 2 h. The solution was cooled to room temperature, and CH_2Cl_2 was removed under reduced pressure. The solid was dried overnight under moderate heating (around 35 °C) and reduced pressure and used without further purification.

4-(*N*,*N*-Bis(4-methoxy-phenyl)amino)-*N*-(4-*tert*-butylphenyl)-benzamide (7). A suspension of **6** (crude prepared from 200 mg of the acid) in 4.5 mL of DMAc was added slowly to a solution of *p*-^{t}Bu-aniline (62 mg, 0.41 mmol) in 0.5 mL DMAc and a few drops of pyridine. The resulting solution was stirred overnight at room temperature. After precipitation with water, the precipitate was chromatographed on silica with CH_2Cl_2 to yield **7** as yellow solid (140 mg, 70%). ^{1}H NMR ($CDCl_3$, 300 MHz): δ 7.72 (bs, 1H, NH); 7.65 (d, 2H, H$_{o1}$, ^3J = 8.8 Hz); 7.53 (d, 2H, H$_{o2}$, ^3J = 8.8 Hz); 7.36 (d, 2H, H$_{m1}$, ^3J = 8.8 Hz); 7.10 (d, 4H, H$_a$, ^3J = 9 Hz); 6.88 (d, 2H, H$_{m1}$, ^3J = 8.8 Hz); 6.87 (d, 4H, H$_b$, ^3J = 9 Hz); 3.81 (s, 6H, CH_3); 1.32 (s, 9H, ^{t}Bu). ^{13}C NMR ($CDCl_3$, 75 MHz): δ 165.2, 167.7, 151.8, 147.1, 139.6, 135.7, 128.2, 127.5, 125.8, 125.1, 119.8, 117.9, 114.9, 55.5, 34.4, 31.4.

Ir(^{t}Butpy)(tpy-diapa)(PF$_6$)$_3$ (10^{3+}). Method A. ^{t}ButpyIrCl$_3$ **8** (40 mg, 0.056 mmol) was dissolved in ethylene glycol (20 mL), and the solution was degassed. Bis(4-methoxyphenyl)(4-[2,2′;6′,2″]terpyridin-4′-ylphenyl)amine **9** (30 mg, 0.056 mmol) was added as a solid, and the solution was degassed again. The reaction flask was placed in an oil bath at160 °C. After 4 min, the temperature reached 180 °C, and after 7 min, the solution was refluxed. After 5 min at reflux, the reaction flask was lifted from the oil bath, and the deep purple solution cooled to room temperature. Aqueous KPF_6 was added, and the resulting precipitate was filtered off. It was chromatographed on silica using acetone/H_2O/KNO_3 as eluent (from 100/0/0 to 100/10/0.5) to give 60 mg of pure **10^{3+}** (68% yield). ^{1}H NMR (acetone-d_6, 400 MHz): δ 9.50 (s, 2H, H$_{3'5'}$); 9.44 (s, 2H, D$_{3'5'}$); 9.13 (d, 2H, D$_{33''}$, ^3J = 7.8 Hz); 9.09 (d, 2H, H$_{33''}$, ^3J = 7.7 Hz); 8.38 (two overlapping ddd, 4H, H$_{44''}$D$_{44''}$, ^3J = 7.9 Hz, ^4J = 1.6 Hz); 8.27 (dd, 2H, D$_{66''}$, ^3J = 5.5 Hz, ^4J = 1 Hz); 8.20 (dd, 2H, H$_{66''}$, ^3J = 5.5 Hz, ^4J = 1 Hz); 8.18 (d, 2H, H$_{m1}$, ^3J = 9.2 Hz); 8.07 (d, 2H, H$_o$, ^3J = 1.9 Hz); 7.87 (t, 1H, H$_p$, ^3J = 1.8 Hz); 7.68−7.60 (m, 4H, H$_{55''}$D$_{55''}$); 7.26 (d, 4H, H$_b$, ^3J = 8.9 Hz); 7.05 (d, 2H, H$_{o1}$, ^3J = 9.0 Hz); 7.04 (d, 4H, H$_a$, ^3J = 9.0 Hz); 3.87 (s, 6H, CH_3); 1.50 (s, 18H, ^{t}Bu). MS (FAB$^+$), *m*/*z* (calcd): 1440.4 (1440.4) [M − PF$_6$]$^+$, 1295.4 (1295.4) [M − 2PF$_6$]$^+$, 1150.4 (1150.5) [M − 3 PF$_6$]$^+$, 647.7 (647.7) [M − 2PF$_6$]$^{2+}$, 575.2 (575.3) [M − 3PF$_6$]$^{2+}$. UV−vis (CH_3CN) λ_{max}/nm (ϵ/M^{-1} cm^{-1}): 506 (19600, CT).

Ir(^{t}Butpy)(tpy-PhNCO−PhNMe$_2$)(PF$_6$)$_3$ (11^{3+}). Method A. ^{t}ButpyIrCl$_3$ **8** (72 mg, 0.1 mmol) was dissolved in ethylene glycol (35 mL), and the solution was degassed. Compound **3** (47 mg, 0.1 mmol) was added as a solid, and the solution was degassed again. The reaction flask was placed in an oil bath at160 °C. After 5 min, the temperature was 180 °C, and after 8 min, reflux was reached. After 5 min at reflux, both reactants were completely dissolved. The solution was maintained at reflux under argon and in the dark for 20 min overall. At room temperature, aqueous KPF_6 was added, and the resulting precipitate was filtered off. The precipitate was chromatographed on silica using acetone/H_2O/KNO_3 as eluent (from

(52) Gilman, H.; Brown, G. E. *J. Am. Chem. Soc.* **1940**, *62*, 3208.

100/0/0 to 100/20/2) to give 94 mg of pure $\mathbf{11}^{3+}$ (62% yield ^{1}H NMR (CD_3CN, 400 MHz): δ 9.08 (s, 2H, $D_{3'5'}$); 9.03 (s, 2H, $H_{3'5'}$); 8.91 (s, 1H, NH); 8.78 (d, 2H, $D_{33''}$, ^3J = 7.7 Hz); 8.73 (d, 2H, $H_{33''}$, ^3J = 7.7 Hz); 8.27−8.16 (m, 8H, $D_{44''}H_{44''}H_{o1}H_{m'}$); 7.98 (d, 2H, H_o, ^4J = 1.8 Hz); 7.92 (d, 2H, H_{o2}, ^3J = 9.2 Hz); 7.86 (t, 1H, H_p, ^4J = 1.8 Hz); 7.72 (d, 2H, $D_{66''}$, ^3J = 5.9 Hz); 7.69 (d, 2H, $H_{66''}$, ^3J = 5.9 Hz); 7.53−7.48 (m, 4H, $D_{55''}H_{55''}$); 6.83 (d, 2H, H_{m2}, ^3J = 9.2 Hz); 3.07 (s, 6H, NMe_2); 1.53 (s, 18H, ^{t}Bu). MS (FAB$^+$), *m*/*z*: 1375.4 [M − PF_6]$^+$, 1230.5 [M − 2PF_6]$^+$, 1085.5 [M − 3PF_6]$^+$, 543.0 [M − 3PF_6]$^{2+}$. UV−vis (CH_3CN) λ_{max}/nm (ϵ/M^{-1} cm^{-1}): 376 (29500), 410 (26900).

Ir(^{t}Butpy)(tpy-PhNH$_2$)(PF$_6$)$_3$ ($\mathbf{12}^{3+}$). Method A. A suspension of ^{t}ButpyIrCl$_3$ **8** (261.3 mg, 0.36 mmol) and **2** (117.8 mg, 0.36 mmol) in ethylene glycol (14 mL) was homogenized by sonication and then refluxed for 5 min under microwave irradiation. The crude material was precipitated with a saturated solution of KPF_6 and filtered off. It was chromatographed on silica using acetonitrile/H_2O/KNO_3 from 100/0/0 to 100/10/0.5 as eluent. After anion exchange from NO_3^- to PF_6^-, $\mathbf{12}^{3+}$ was obtained as a dark red solid. Yield 85% (425 mg). ^{1}H NMR (CD_3CN; 200 MHz): δ 9.02 (s, 2H, $H_{3'5'}$); 8.95 (s, 2H, $D_{3'5'}$); 8.79−8.68 (m, 4H, $H_{33''}D_{33''}$); 8.27−8.18 (m, 4H, $H_{44''}D_{44''}$); 8.07 (d, 2H, H_{o1}, ^3J = 8,7 Hz); 7.97 (d, 2H, H_o, ^4J = 1.7 Hz); 7.85 (t, 1H, H_p, ^4J = 1.7 Hz); 7.73−7.66 (m, 4H, $H_{66''}D_{66''}$); 7.52−7.44 (m, 4H, $H_{55''}D_{55''}$); 6.98 (d, 2H, H_{m1}, ^3J = 8.8 Hz); 5.06 (s, 2H, NH_2); 1.52 (s, 18H, ^{t}Bu). ES$^+$-MS, *m*/*z*: 1228.4 [M − PF_6 + H]$^+$, 541.7 [M − 2PF_6]$^{2+}$, 312.8 [M − 3PF_6]$^{3+}$. UV−vis (CH_3CN) λ_{max}/nm (ϵ/M^{-1} cm^{-1}): 253 (19300); 281 (17300); 302sh (16500); 451 (7300).

Ir(^{t}Butpy)(tpy-PhNHCO-diapa)(PF$_6$)$_3$ ($\mathbf{13}^{3+}$). Method B. Compound **6** (crude material prepared from 210 mg of **5**) was added slowly to a solution of $\mathbf{12}^{3+}$ (72 mg, 0.052 mmol) in 1 mL of DMAc and 0.5 mL of pyridine. The resulting solution was stirred for 4 h. After precipitation with water/KPF_6, the crude was chromatographed on silica with acetonitrile/H_2O/KNO_3 from 100/0/0 to 100/6/0.6 as eluent. After anion exchange, $\mathbf{13}^{3+}$ was obtained as a yellow solid with 60% yield (53 mg). ^{1}H NMR (CD_3CN; 200 MHz): δ 9.08 (s, 2H, $D_{3'5'}$); 9.03 (s, 2H, $H_{3'5'}$); 9.00 (s, 1H, NH); 8.76 (bd, 2H, $D_{33''}$, ^3J = 6.1 Hz); 8.73 (bd, 2H, $H_{33''}$, ^3J = 6.1 Hz); 8.26−8.21 (m, 6H, $H_{44''}D_{44''}H_{o1}$); 8.15 (d, 2H, H_{m1}, ^3J = 6.7 Hz); 7.97 (d, 2H, H_o, ^4J = 1.3 Hz); 7.85 (t, 1H, H_p, ^4J = 1.3 Hz); 7.82 (d, 2H, H_{o2}, ^3J = 6.8 Hz); 7.70 (bd, 2H, $D_{66''}$, ^3J = 6.6 Hz); 7.69 (bd, 2H, $H_{66''}$, ^3J = 6.6 Hz); 7.52−7.48 (m, 4H, $H_{55''}D_{55''}$); 7.19 (d, 4H, H_a, ^3J = 6.8 Hz); 6.97 (d, 4H, H_b, ^3J = 6.8 Hz); 6.82 (d, 2H, H_{m2}, ^3J = 6.8 Hz); 3.80 (s, 6H, CH_3); 1.51 (s, 18H, ^{t}Bu). SM (API-ES), *m*/*z* (calcd): 1559.5 (1559.4) [M − PF6]$^+$; 707.3 (707.2) [M − 2PF6]$^{2+}$; 423.2 (423.2) [M − 3PF_6]$^{3+}$. UV−vis (CH_3CN) λ_{max}/nm (ϵ/M^{-1} cm^{-1}): 252 (58700); 278 (56800); 322 (55200); 376 (34800).

Ir(^{t}Butpy)(tpy-PhNHCO−Ph)(PF$_6$)$_3$ ($\mathbf{14}^{3+}$). Method B. Compound $\mathbf{12}^{3+}$ (51.6 mg, 0.037 mmol) was dissolved in DMAc (3 mL) and pyridine. (1.5 mL). Benzoyl chloride (120 mg, 0.86 mmol, large excess) was added, and the solution was stirred at room temperature for 2 h, during which it turned from red to deep yellow. The crude material was precipitated with a saturated solution of KPF_6 and filtered off. It was chromatographed on silica using acetonitrile/H_2O/KNO_3 from 100/0/0 to 100/10/1 as eluent. After anion exchange from NO_3^- to PF_6^-, $\mathbf{14}^{3+}$ was obtained as a yellow solid. Yield 64% (36 mg). ^{1}H NMR (CD_3CN; 400 MHz): δ 9.16 (s, 1H, NH); 9.09 (s, 2H, $D_{3'5'}$); 9.03 (s, 2H, $H_{3'5'}$); 8.78 (d, 2H, $H_{33''}$, ^3J = 6.1 Hz); 7.73 (d, 2H, $D_{33''}$, ^3J = 6.1 Hz); 8.29−8.22 (m, 6H, $H_{44''}D_{44''}H_{o1}$); 8.19 (d, 2H, H_{m1}, ^3J = 6.7 Hz); 8.03 (dd, 2H, H_{o2}, ^3J = 6.1 Hz, ^4J = 1 Hz); 7.98 (d, 2H, H_o, ^4J = 1.3 Hz); 7.86 (t, 1H, H_p, ^4J = 1,3 Hz); 7.73−7.69 (m, 4H, $H_{66''}D_{66''}$); 7.66 (d, 1H, H_{p2}, ^3J = 5.6 Hz); 7.60 (t, 2H, H_{m1}, ^3J = 5.6 Hz); 7.53−7.49 (m, 4H, $H_{55''}D_{55''}$); 1.53 (s, 18H, ^{t}Bu). SM (MALDI-TOF), *m*/*z* (calcd): 1041.9 (1042.3) [M − 3PF_6]$^+$. UV−vis (CH_3CN) λ_{max}/nm (ϵ/M^{-1} cm^{-1}): 253 (53600); 281 (52300); 354 (27500); 379 (30000).

Photophysical Determinations. Spectroscopic grade solvents (C. Erba) were used without further purification. Absorption spectra were recorded with a Perkin-Elmer Lambda 9 spectrophotometer, and uncorrected emission spectra were detected by a Spex Fluorolog II spectrofluorimeter. Relative luminescence intensities were evaluated from the area (on an energy scale) of the luminescence spectra corrected for the photomultiplier response. Luminescence quantum yields ϕ for the model **Ir−1** were obtained with reference to a standard, Ir(III)(4′-tolyl −2,2′:6′,2″-terpyridine)$_2$(PF $_6$)$_3$, with Φ_{em} = 0.029 in air saturated acetonitrile.[30] The standard used to determine the luminescence quantum yield for the components in **Ir−D** was either **Ir−1** excited at 430 nm, or D excited at 337 nm. Compound $\mathbf{7}^+$, used as a model of $\mathbf{D}^+$, was generated by the addition of one drop of Br_2 in the solution of **7** in acetonitrile. The molar absorption coefficient was estimated by assuming a complete conversion of the starting material after a few minutes of stirring.

The time resolved luminescence apparatus was based on a Nd:YAG laser (35 ps pulse duration, 355 nm, 1 mJ) and a streak camera; the overall resolution is 20 ps. Lifetimes longer than 2 ns were detected with a time correlated single photon counting apparatus with 1 ns resolution. Transient absorbance in the picosecond range made use of a pump and probe system based on a Nd:YAG laser (35 ps pulse, 355 nm, 3−4 mJ) and an OMA detector. The instrumental response profile was obtained by measuring the buildup of the absorption of the model Ir at 770 nm. Further details on the instrumental setup can be found elsewhere.[53] Transient absorbances in the 20−1000 μs range were determined by a laser flash photolysis apparatus with a Nd:YAG laser (18 ns pulse, 355 nm, 2−4 mJ). Experiments were conducted at 298 K in air equilibrated solutions if not otherwise specified. For luminescence experiments at 77 K, quartz capillary tubes were immersed in liquid nitrogen contained in a homemade quartz Dewar flask.

Experimental uncertainties are estimated to be within 10% for lifetime determination, 15% for quantum yields, 20% for molar absorption coefficients, and 3 nm for emission and absorption peaks.

Acknowledgment. This work was supported by CNRS (France) and by CNR (Italy). L.F. and B.V. thank Ministero dell'Istruzione, dell'Universita' e della Ricerca (FIRB, RBNE019H9K), for support, and E.B. and I.M.D. acknowledge support from the French Ministry of Education.

Supporting Information Available: Proton indexation of the compounds. This material is available free of charge via the Internet at http://pubs.acs.org.

IC0351038

(53) Flamigni, L.; Talarico, A. M.; Serroni, S.; Puntoriero, F.; Gunter, M. J.; Johnston, M. R.; Jeynes, T. P. *Chem. Eur. J.* **2003**, *9*, 2649.